Unbinding of mutually avoiding random walks and two dimensional quantum gravity

Enrico Carlon[1] and Marco Baiesi[2]

[1]*Interdisciplinary Research Institute c/o IEMN, Cité Scientifique BP 69, F-59652 Villeneuve d'Ascq, France*
[2]*INFM Dipartimento di Fisica, via Marzolo 8, I-35131 Padova, Italy*
(Dated: February 2, 2008)

We analyze the unbinding transition for a two dimensional lattice polymer in which the constituent strands are mutually avoiding random walks. At low temperatures the strands are bound and form a single self-avoiding walk. We show that unbinding in this model is a strong first order transition. The entropic exponents associated to denatured loops and end-segments distributions show sharp differences at the transition point and in the high temperature phase. Their values can be deduced from some exact arguments relying on a conformal mapping of copolymer networks into a fluctuating geometry, i.e. in the presence of quantum gravity. An excellent agreement between analytical and numerical estimates is observed for all cases analized.

I. INTRODUCTION

The unbinding transition from a low temperature double stranded polymer to a high temperature single stranded phase has been the subject of recent attention in the context of studies of DNA denaturation [1, 2, 3, 4, 5, 6]. Two main approaches have been used to model this unbinding. The first one relies on the use of directed polymers, where only the transversal coordinate measuring the distance between homologous base pairs is considered [1, 7]. In a second approach, one considers the polymer as being composed of an alternating sequence of double stranded segments and denatured loops [2, 8]. The statistical weights assigned to loops and segments can be estimated using concepts of homopolymers and self-avoiding walks (SAW) statistics.

Traditionally, in the latter class of models, the statistical weight of a loop was approximated as the number of configurations for a closed SAW, neglecting any excluded volume interaction with the rest of the chain [9]. More recently, statistical mechanical ideas based on the theory of polymer networks [10], were used to take into account the excluded volume effects in an approximated way [2]. Although quite simple, this analysis, which was carried out analytically, captures quantitatively very well the asymptotic form of the loop partition function, as a series of numerical investigations on two and three dimensional lattice models have shown [5, 11]. Despite the general good agreement between analytical predictions and simulations, quite small but systematic deviations between the two were found [11].

The aim of this paper is to investigate further on these issues for other types of models of polymer unbinding. We focus on a two dimensional lattice model for which we obtain a series of analytical predictions based on exact results from conformal invariance [12]. In this model, the two constituent strands are two random walks (RWs) with an attractive interaction. While we relax the excluded volume interactions within each strand, mutual avoidance, i.e. the non-overlapping condition between the strands is preserved. This makes the bound dou-

ble stranded state to behave as a SAW, assigning to it a quite different physics compared to that of loops. We show that in this model unbinding is a very strong first order transition.

As is well-known from polymer physics, the partition function of a closed SAW of total length l assumes the following asymptotic form [13]

$$Z(l) \sim \mu^l l^{-c_0} \qquad (1)$$

where μ is a geometric factor and c_0 a universal exponent which equals $c_0 \approx 1.76$ [9] in three dimensions. It has been shown [2] that a loop attached to two long segments or loops (see Fig. 1) has still a partition function of the form of Eq. (1), but with different exponents. For instance in three dimensions one finds for a loop embedded between two long segments [2] $c_{ss} \approx 2.1$ and $c_{ll} \approx 2.2$ for a loop embedded between two long loops (here we used the subscripts s or l to indicate neighboring segments or loops). An increase of c for embedded loops is caused by the tendency of the loop to become more "localized" due to excluded volume interactions with the rest of the chain. For $c > 2$ the transition becomes first order [8, 9].

In this paper we calculate analytically the values of the exponents c_{ll} and c_{ss}, as well as other type of entropic exponents, for the model of mutually avoiding random walks. The calculation relies on conformal mapping of copolymer networks into a fluctuating geometry [12],
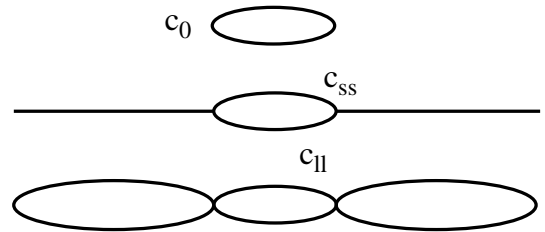

FIG. 1: Hierarchy of exponents describing the loop entropy for an isolated loop (c_0), a loop embedded between two long segments (c_{ss}) and a loop embedded between two long loops (c_{ll}).
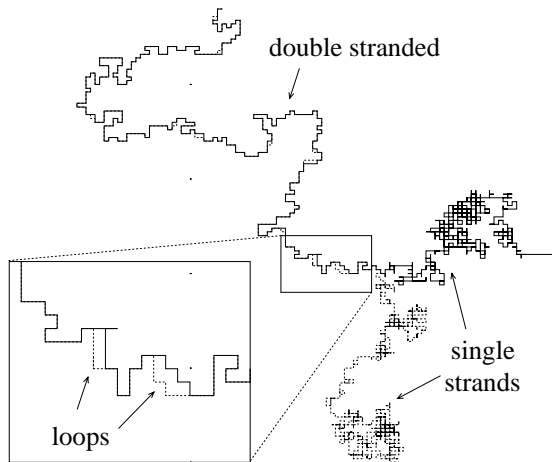
FIG. 2: Snapshot of a configuration for the model studied in this paper generated by the Pruned Enriched Rosenbluth Method (PERM). The two walks are indicated as solid and dashed lines. When they are bound only the solid line is visible. Inset: Blow up of a small area of double stranded phase with two embedded loops. The loops are oriented, i.e. following the direction of one of the strands, the other strands is always found on the same side.

i.e. in the presence of quantum gravity. This theory, which was recently applied to the calculation of multi-fractal spectra of harmonic measures [17], enables one to obtain exact entropic exponents of networks composed of arbitrary mixtures of random and self-avoiding walks [12]. We also performed a series of Monte Carlo simulations in order to determine the numerical values for the exponents. In all cases analyzed the numerical and analytical results are in excellent agreement. This is due, as we will discuss below, to the strong first order nature of the unbinding transition, which makes the model an ideal testground where copolymer network theories can be applied.

Part of the results presented here, have been discussed in concise form in Ref. [14]. In this paper we present the results of large scale numerical calculations, which we extend to other quantities not considered previously, and present a full account of the analytical results. The present model has also been investigated by means a continuum approach [4], in which mutual avoidance between the two strands has been approximated by an effective long-range interaction, an approach which predicts a first order unbinding transition.

II. THE MODEL

We consider two random walks of length N on a square lattice described by the vectors $\vec{r}_1(k)$ and $\vec{r}_2(k)$ with $k = 0, 1 \ldots N$. The walks have common origin $\vec{r}_1(0) = \vec{r}_2(0)$ and are not allowed to overlap except at homologous sites, i.e. $\vec{r}_1(i) = \vec{r}_2(j)$ is possible only if $i = j$. Whenever such a contact is realized the sys-
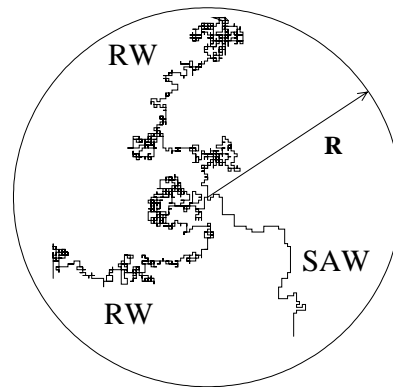

FIG. 3: Example of a star copolymer formed by two random walks and a self-avoiding walk, where all three of them are mutually avoiding and have average size equal to R. The exact entropic exponent for any star copolymer with an arbitrary number of random and self-avoiding walks can be calculated thanks to a mapping onto a fluctuating geometry (see Sec. III).

tem gains an energy $\varepsilon = -1$. At very low temperatures the two walks are fully bound and form a self-avoiding walk, since, as the walks are mutually avoiding, a bound site $\vec{r}_1(i) = \vec{r}_2(i)$ cannot overlap any other sites on both strands. At higher temperatures unbinding starts from the unconstrained edge $i = j = N$ and loops proliferate along the chain. Figure 2 shows a snapshot of a configuration generated by the Pruned Enriched Rosenbluth Method (PERM) [15], where the two strands are represented by solid and dashed lines, respectively. Notice that the double-stranded part has a characteristic self-avoiding walk behavior and the unbound single strands behave as mutually avoiding random walks. The inset of Fig. 2 shows a blow-up of part of the double stranded chain with two short loops of few lattice spacings of length. The model is constructed such that following the two strands $\vec{r}_1(k)$ and $\vec{r}_2(k)$ from the origin $k = 0$ to $k = N$ one finds one of the two strands (say $\vec{r}_1(k)$) when unbound always at the left side of the other strand, i.e. the loops are oriented. This choice will allow us to restrict the type of diagrams considered in the continuum polymer network description of the model.

III. CONFORMAL MAPPING ONTO TWO DIMENSIONAL QUANTUM GRAVITY

A. Star copolymers

Duplantier formulated an elegant theory [12] which allows one to compute exact entropic exponents for star copolymers, an example of which is shown in Fig. 3. A star copolymer is formed by an arbitrary mixture of random and self-avoiding walks joined at a common origin, which can be all mutually avoiding (as in the example of Fig. 3) or partially transparent to each other.

One is typically interested in the grand-canonical partition function $Z_R(S)$, for a star S formed by f_1 self-avoiding walks (SAWs) and f_2 random walks (RWs), all with average size R from the origin of the star, R denoting the end-to-end distance for each walk. Having the same size, SAWs and RWs are characterized by different lengths, scaling as $\sim R^{1/\nu}$, with $\nu = 3/4$ for a SAW and $\nu = 1/2$ for a RW. Fugacities per unit of step length are associated to each type of walk. By tuning their values appropriately both walks become critical. In this limit the partition function scales asymptotically for large R as [12]

$$Z(S) \sim R^{\eta(S) - f_1 \eta_2}, \qquad (2)$$

where $\eta(S)$ is the scaling exponent associated to the singularity at the center of the star and η_2 the entropic exponent associated to an isolated SAW ($\eta_2 = -11/24$ in two dimensions, while the corresponding exponent for RWs is zero). We have followed here the notation of Ref. [16], which is slightly different from that of the original work of Duplantier [12], but more suitable for a generalization to networks. The star exponent can be written in the following form:

$$\eta(S) = -2\Delta(S) + f_1 \frac{\eta_\phi}{2}, \qquad (3)$$

with $\Delta(S)$ the conformal scaling dimension and $\eta_\phi = 5/24$ the correlation length exponent [16].

Here we review briefly the main formulas leading to the exact value of the exponent $\Delta(S)$ for an arbitray star copolymer S. Details of the derivation can be found in the Refs. [12, 17]. The main idea is to map the star copolymer from the planar euclidean geometry onto a two dimensional random lattice, i.e. in the presence of *quantum gravity*.

Besides the bulk scaling dimension $\Delta(S)$ of a star S we will also consider star copolymers confined in a half-plane with the origin near the boundary of the plane, which defines the surface scaling dimension $\widetilde{\Delta}(S)$. We use the notations $\Delta^{\text{qg}}(S)$ and $\widetilde{\Delta}^{\text{qg}}(S)$ for bulk and surface conformal dimensions in the random lattice (here qg stands for quantum gravity). Given two walks A and B, with a common origin we indicate (as in Ref. [12]) with the symbol $A \vee B$ a star configuration where the two walks are allowed to overlap each other and with $A \wedge B$ a configuration where A and B are non-overlapping.

The main result of the theory is that in the fluctuating geometry the surface conformal dimensions for two mutually avoiding walks are additive [12] i.e.:

$$\widetilde{\Delta}^{\text{qg}}(A \wedge B) = \widetilde{\Delta}^{\text{qg}}(A) + \widetilde{\Delta}^{\text{qg}}(B). \qquad (4)$$

For transparent walks in the plane, due to the trivial factorization of their partition functions one has:

$$\widetilde{\Delta}(A \vee B) = \widetilde{\Delta}(A) + \widetilde{\Delta}(B). \qquad (5)$$

We point out to a sort of duality between Eqs. (4) and (5). Eq. (4) states that non-intersecting walks, become
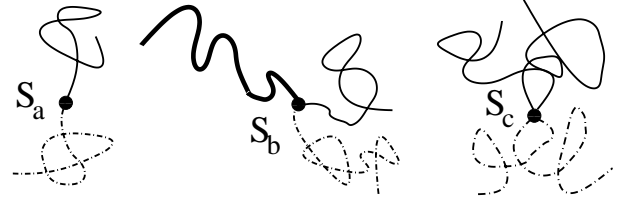

FIG. 4: Star copolymers considered in this paper. Thin lines denote random walks, while thick lines denote self-avoiding walks. Solid and dashed thin lines are allowed to overlap with thin lines of the same species, but not allowed to overlap thin lines of the other species (eg. overlap between solid and dashed thin lines is not allowed). The conformal scaling dimensions for the examples in the figure are $\Delta(S_a) = 5/8$, $\Delta(S_b) = 39/32$ and $\Delta(S_c) = 35/24$ (see text).

transparent to each other when placed in a fluctuating geometry. The Eqs. (4) and (5) can be generalized to any nested star copolymer structure (see Ref. [12]).

Conformal invariance relates the bulk and surface scaling dimensions in the two geometries as [12]:

$$\Delta = U(\Delta^{\text{qg}}), \qquad (6)$$

$$\widetilde{\Delta} = U(\widetilde{\Delta}^{\text{qg}}), \qquad (7)$$

where $U(x) = \frac{x}{3}(1 + 2x)$ and the inverse $U^{-1}(x) = \frac{1}{4}(\sqrt{24x + 1} - 1)$. The previous equations follow from the work of Knizhnik, Polyakov and Zamolodchikov [18], who established the existence of a relation between the conformal dimensions of scaling operators in the plane and those in the presence of gravity. Finally the relation

$$\widetilde{\Delta}^{\text{qg}} = 2\Delta^{\text{qg}} + \frac{1}{2}, \qquad (8)$$

connects surface and bulk conformal dimensions in the fluctuating geometry and can be derived from some factorization properties of star partition functions under quantum gravity [19].

For random and self-avoiding walks the conformal dimensions are [12]:

$$\widetilde{\Delta}_{\text{RW}} = 1, \quad \widetilde{\Delta}^{\text{qg}}_{\text{RW}} = 1, \quad \Delta_{\text{RW}} = \frac{1}{8}, \quad \Delta^{\text{qg}}_{\text{RW}} = \frac{1}{4}, \quad (9)$$

$$\widetilde{\Delta}_{\text{SAW}} = \frac{5}{8}, \quad \widetilde{\Delta}^{\text{qg}}_{\text{SAW}} = \frac{3}{4}, \quad \Delta_{\text{SAW}} = \frac{5}{96}, \quad \Delta^{\text{qg}}_{\text{SAW}} = \frac{1}{8}. \quad (10)$$

As a practical example of the use of the above formulas we calculate the conformal dimensions of the three star copolymers shown in Fig. 4, which are the configurations relevant for the model discussed in this paper.

Let us consider first the star copolymer composed by two mutually avoiding random walks (i.e. S_a of Fig. 4). The equation (4) states that the surface conformal dimension in the fluctuating geometry for two mutually avoiding walks is additive, thus for S_a it is twice as large as that of a random walk

$$\widetilde{\Delta}^{\text{qg}}(S_a) = 2\widetilde{\Delta}^{\text{qg}}_{\text{RW}} = 2. \qquad (11)$$

From Eq. (8) one finds therefore for the bulk dimension in the fluctuating geometry: $\Delta^{\mathrm{qg}}(S_a) = 3/4$. The final step to obtain the bulk dimension in the plane is to use the conformal mapping [Eq. (6)] which yields

$$\Delta(S_a) = U(3/4) = \frac{5}{8}. \qquad (12)$$

The generalization to k mutually avoiding random walks is given in the Appendix A. The above derivation of $\Delta(S_a)$ illustrates the general strategy of the calculation: the conformal dimension is first calculated in the fluctuating geometry, where mutual avoidance is easy to implement [see Eq. (4)] and then obtained for the planar geometry from Eqs. (6) and (7).

For the star formed by two random walks and a self-avoiding walk all of them avoiding each other (S_b of Fig. 4), one proceeds along the same lines as done for S_a. First, the additivity of surface scaling dimensions in the fluctuating geometry [Eq. (4)] implies that $\widetilde{\Delta}^{\mathrm{qg}}(S_b) = 2\widetilde{\Delta}^{\mathrm{qg}}_{\mathrm{RW}} + \widetilde{\Delta}^{\mathrm{qg}}_{\mathrm{SAW}} = 11/4$. Therefore, for the bulk dimension one finds [Eq. (8)]: $\Delta^{\mathrm{qg}}(S_b) = 9/8$. Finally, the conformal mapping [Eq. (6)] yields:

$$\Delta(S_b) = U(9/8) = \frac{39}{32}. \qquad (13)$$

For the star copolymer S_c of Fig. 4 the calculation is slightly different. Both solid and dashed walks are transparent to each other, therefore we first need to calculate the scaling dimension for the sub-star composed either by solid or by dashed lines only. Two transparent random walks (RW_1 and RW_2) in the planar geometry have additive surface conformal dimension [Eq. (5)] thus

$$\widetilde{\Delta}(\mathrm{RW}_1 \vee \mathrm{RW}_2) = 2\widetilde{\Delta}_{\mathrm{RW}} = 2. \qquad (14)$$

By inversion of Eq. (7), we obtain the corresponding surface conformal dimension in the fluctuating geometry: $\widetilde{\Delta}^{\mathrm{qg}}(\mathrm{RW}_1 \vee \mathrm{RW}_2) = U^{-1}(2) = 3/2$. Now, as in the fluctuating geometry the two scaling dimensions of the mutually avoiding dashed and solid sub-stars are additive one finds from Eq. (4): $\widetilde{\Delta}^{\mathrm{qg}}(S_c) = 2\widetilde{\Delta}^{\mathrm{qg}}(\mathrm{RW}_1 \vee \mathrm{RW}_2) = 3$. Eq. (8) yields for the bulk: $\Delta^{\mathrm{qg}}(S_c) = 5/4$. The final step is the mapping back into the planar geometry [Eq.(6)] which yields:

$$\Delta(S_c) = U(5/4) = \frac{35}{24}. \qquad (15)$$

B. Networks with arbitrary topology

We consider now exponents associated to networks of arbitrary topology, formed by mixtures of RWs and SAWs connected to each other in such a way to form loops and dangling ends (examples are shown in Fig. 5 and 6). The partition function for a network G containing f_1 SAWs, in the limit when all walks are critical takes
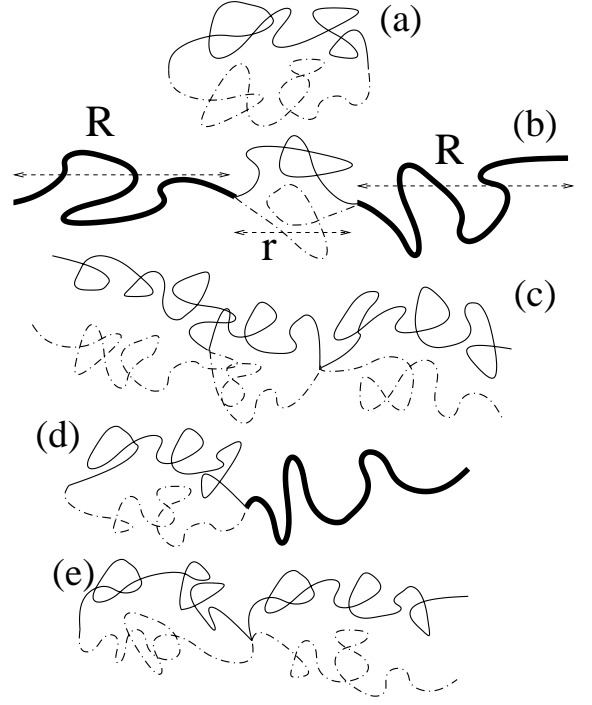

FIG. 5: Examples of loop configurations relevant for the model. (a) Isolated loop formed by two mutually avoiding random walks, (b) loop embedded between long SAWs ($R \gg r$), (c) Loop embedded between two other long loops. At the edges the first loop formed at the origin of the two walks can be attached to a long SAW (d) or to another long loop (e).

the form [16]

$$Z(G) \sim R^{\eta_G - f_1 \eta_2}, \qquad (16)$$

where the universal exponent η_G depends on the topology of G as follows [20]

$$\eta_G = -d\mathcal{L} + \sum_S n_S \eta(S) \qquad (17)$$

where d is the dimensionality of the system ($d = 2$ in this paper), $\mathcal{L}$ the number of independent loops and the sum is extended to all constituent vertices forming the network, each contributing for a factor $\eta(S)$ (the star exponent defined by Eqs. (3) and (2), and n_S is the degeneracy of the vertex S. Using the results of the preceding section and recalling that for a vertex S with f_1 outgoing SAWs one has $\eta(S) = -2\Delta(S) + f_1 \eta_\phi/2$ [Eq. (3)] we can now calculate the network exponents for the examples in Fig. 5 and 6, which are those relevant for the unbinding transition considered in this paper.

For the isolated loop of Fig. 5(a) one has $\mathcal{L} = 1$ and there are two vertices S_a, as defined in Fig. 4. As there are no SAWs $f_1 = 0$ in Eqs. (16) and (3) therefore Eqs. (17) and (12) imply that

$$\eta_G = -2 - 2\eta(S_a) = -2 - 4\Delta(S_a) = -2 - \frac{5}{2} \qquad (18)$$

Usually we are interested in the scaling as function of the loop length, and not of its radius of gyration, therefore the partition function is:

$$Z_{\text{loop}} \sim l^{\nu \eta_G} \sim l^{-c_0} \qquad (19)$$

with $\nu = 1/2$ for random walks and where we have introduced the entropic exponent for an isolated loop, in analogy as what discussed in the Introduction. We have $c_0 = 2 + 1/4 = 2.25$. Differently from the case of self-avoiding loops (see Introduction) in the present model already at the level of an isolated loop $c_0 > 2$, implying that the first order character of the transition is rather strong, as remarked in Ref. [11].

Equation (16) can be generalized to the case where the network is formed by walks of different sizes, say R and r. In this case the network partition function becomes:

$$Z(G) \sim R^{\eta_G - f_1 \eta_2} f\left(\frac{r}{R}\right) \qquad (20)$$

with f a scaling function. In all the other cases (Fig. 5(b-e)) we will consider the limit in which r, the size of the loop, is much smaller than R the size of the walks or loops attached to it.

We consider now the network of Fig. 5(b) which contains one loop $\mathcal{L} = 1$ and two vertices S_b (as in Fig. 4) therefore:

$$\eta_G - 2\eta_2 = -2 + 2\left[-2\Delta(S_b) + \frac{\eta_\phi}{2} - \eta_2\right] \qquad (21)$$

In the limit $r \ll R$ one should recover the partition function of a single SAW ($\sim R^{-\eta_2}$), which implies that the scaling function of Eq. (20) behaves as

$$f(x) \sim x^{-2-4\Delta(S_b)+\eta_\phi-\eta_2} \qquad \text{for} \quad x \to 0 \qquad (22)$$

In this limit the partition function of the network becomes:

$$Z(G) \sim R^{-\eta_2} r^{-2-4\Delta(S_b)+\eta_\phi-\eta_2} \qquad (23)$$
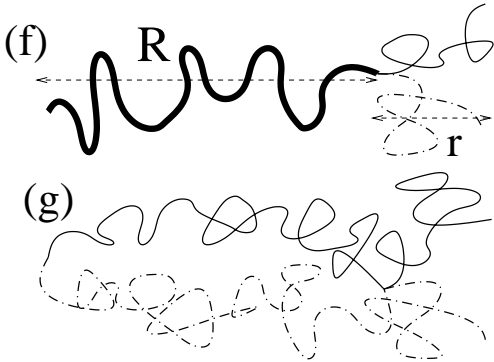

FIG. 6: Configurations of end-segments linked to a long SAW (a) and to a loop formed by two mutually avoiding random walks (b).

and thus factorizes as $Z(G) \sim Z_{\text{SAW}} Z_{\text{loop}}$, i.e. in a contribution from a long SAW and of a loop. The latter expressed in terms of its total length l reads:

$$Z_{\text{loop}} \sim l^{-\nu[2+4\Delta(S_b)-\eta_\phi+\eta_2]} \sim l^{-c_{\text{ss}}} \qquad (24)$$

Using the numerical values of the exponents given in the preceding section we find: $c_{\text{ss}} = 3 + 5/32$ [21]. Note that the derivation of Eq. (24) is similar to that for the unbinding of SAWs reported in Ref. [2].

The next example is the configuration of Fig. 5(c), i.e. a loop confined between two other long loops. As the calculation of its partition function follows closely that of a loop confined between two SAWs we report here the final result:

$$Z_{\text{loop}} \sim l^{-\nu[2+2\Delta(S_c)]} \sim l^{-c_{\text{ll}}}, \qquad (25)$$

and thus from Eq. (15) we find: $c_{\text{ll}} = 2 + 11/24$. Notice that $c_{\text{ll}} < c_{\text{ss}}$, contrary to what happens for self-avoiding walks [2]. This follows from the random walks character for isolated strands: As solid and dashed lines in Fig. 5(c) are allowed to overlap themselves a loop bounded by two loops is "less localized" (smaller c) than a loop bounded by two SAWs.

We will also be interested in the statistical properties of the first loop formed at the common origin of the two walks, therefore we consider also the case of a loop bound to the rest of the polymer only on one edge (see Fig. 5(d-e)). Also in this case we only report the final results as the calculation follows the example above. For the partition function of a loop bound to a long segment (Fig. 5(d)) we find

$$Z_{\text{loop}} \sim l^{-\nu[2+2\Delta(S_a)+2\Delta(S_b)-\eta_\phi/2]} \sim l^{-c_{\text{s}}} \qquad (26)$$

with $c_{\text{s}} = 2 + 19/24$ while for a loop attached to a long loop (Fig. 5(e)) we find:

$$Z_{\text{loop}} \sim l^{-\nu[2+2\Delta(S_c)]} \sim l^{-c_{\text{l}}} \qquad (27)$$

with $c_{\text{l}} = 2 + 11/24$. Notice that, curiously, $c_{\text{l}} = c_{\text{ll}}$ a relation which is not valid only for this particular model, but it is quite general for all polymer unbinding transitions, wether the constituents strands are SAWs or mutually avoiding RWs.

Finally besides loops it is also interesting to consider end-segments distributions, i.e the length of the single strands at the free end of the polymer (see Fig. 6), as done for the SAWs in Ref. [22]. Again, as the calculation is very similar to those reported in this section we only give the final results. For end segments each of length n bounded to a SAW of size R, in the limit $R \gg r$, with r the size of the end-segments ($r \sim n^{1/2}$) we find:

$$Z_{\text{end}} \sim n^{-\nu[2\Delta(S_b)-\eta_\phi/2]} \sim n^{-\gamma_s} \qquad (28)$$

where we have introduced a new exponent equal to $\gamma_s = 7/6$.

TABLE I: Summary of the exact loop and end-segments entropic exponents for the configurations of Fig. 5 and 6.

	Loops		End segments
c_0	$2 + 1/4 \; (\approx 2.25)$	γ_0	$5/8 \; (\approx 0.62)$
c_{ss}	$3 + 5/32 \; (\approx 3.16)$	γ_s	$7/6 \; (\approx 1.17)$
c_{ll}	$2 + 11/24 \; (\approx 2.46)$	γ_l	$5/6 \; (\approx 0.83)$
c_s	$2 + 19/24 \; (\approx 2.79)$		
c_l	$2 + 11/24 \; (\approx 2.46)$		

Similarly for the configuration of Fig. 6(g) we find

$$Z_{\text{end}} \sim n^{-\nu[2\Delta(S_c)-2\Delta(S_a)]} \sim n^{-\gamma_l} \qquad (29)$$

with $\gamma_l = 5/6$. Notice that analogously as what we have found for the loops, also the end-segments bound to a long loop are less localized than those bound to a SAW ($\gamma_l < \gamma_s$).

The results obtained in this Section are summarized in Table I, to which we have also added γ_0 the exponent associated to isolated end-segments. This exponent is associated to the configuration of Fig. 4(a), therefore: $\gamma_0 = 2\nu\Delta(S_a) = 5/8$.

IV. NUMERICAL RESULTS

Polymer configurations in which each strand is of length $N = 1280$ were generated by the Pruned Enriched Rosenbluth Method (PERM) which is described in Ref. [15]. We performed first three runs at fixed tem-

FIG. 7: (a) Plot of the specific heat peaks heights $C_{\max}$ as a function of the chain length N on a log-log scale. From a linear fit and by Eq. (30) we find as estimate of the crossover exponent $\phi = 1.000(2)$. (b) Plot of the inverse temperature position of the peaks as function of $1/N$.

peratures around the critical point and used the multi-hystogram method [23] to interpolate results to arbitrary temperatures in the transition region. A precise estimate of the transition point was obtained by the analysis of the specific heat maximum per unit of length $C_{\max}(N)$, which is expected to scale as function of the chains length N as [13]

$$C_{\max}(N) \sim N^{2\phi-1} \qquad (30)$$

a relation which defines the crossover exponent ϕ. Figure 7(a) shows a plot of the peak heights $C_{\max}(N)$ as a function of the chain length N on a log-log scale. A linear fit of the data yields $\phi = 1.000(2)$ in excellent agreement with a first order transition, for which one expects $\phi = 1$ [13]. The sharp determination of ϕ is a signature of a rather strong first order character of the transition. It is interesting to point out that in the case of unbinding of self-avoiding walks, although the transitions is known to be of first order type, it is difficult to extrapolate an exponent ϕ which is consistent with $\phi = 1$ [3, 5] (at least in three dimensions).

The peak position is expected to scale as

$$\beta_{\max}(N) \sim \beta_c + \frac{A}{N^\phi} \qquad (31)$$

with A a constant. The first order character ($\phi = 1$) is confirmed by the scaling of the peak positions, as illustrated in Fig. 7(b) which shows a plot of $\beta_{\max}(N)$ vs. $1/N$ (β is the inverse temperature). We performed a series of iterated linear fits of $\beta_{\max}(N)$ vs. $1/N$ and obtained the following estimate of the transition point $\beta_c = 1.7617(1)$.

A. Behavior at the transition point $\beta = \beta_c$

We focus first on the behavior at the transition point $\beta = \beta_c = 1.7617$. The probability distribution of finding a loop of length l is expected to decay as a function of l as [5]

$$P(l) \sim l^{-c}, \qquad (32)$$

from which the exponent c can be calculated. Figure 8(a) shows a log-log plot of $P(l)$ versus l for $N = 1280$ at β_c. As a comparison we plot, as straight lines, the slopes corresponding to the analytical estimates of the exponents c_{ss} and c_{ll}, for a loop embedded between two segments and two loops, respectively, calculated in the preceding section. Notice the excellent agreement of the numerical results with the decay exponent c_{ss}, which indicates that considering each loop as simply bounded by pure SAWs approximates extremely well the polymer configuration at the transition point. As $P(l)$ decays rather fast in l ($\sim l^{-c}$ with $c \approx 3.2$), rather long runs are needed in order to obtain an accurate statistics.

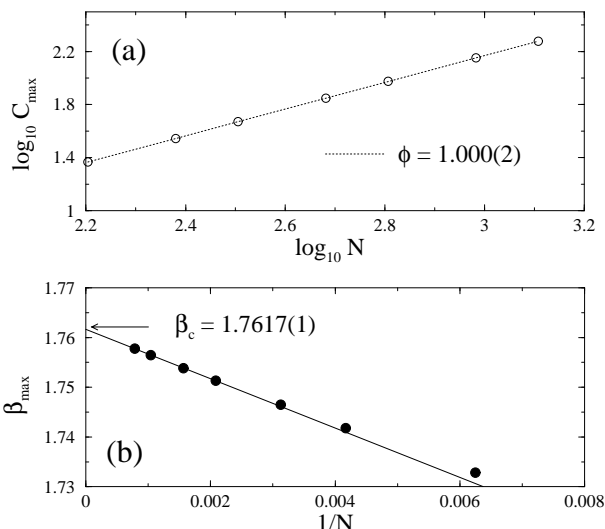We have also analyzed the probability distribution of the first loop $P_0(l)$, which is formed at the common origin
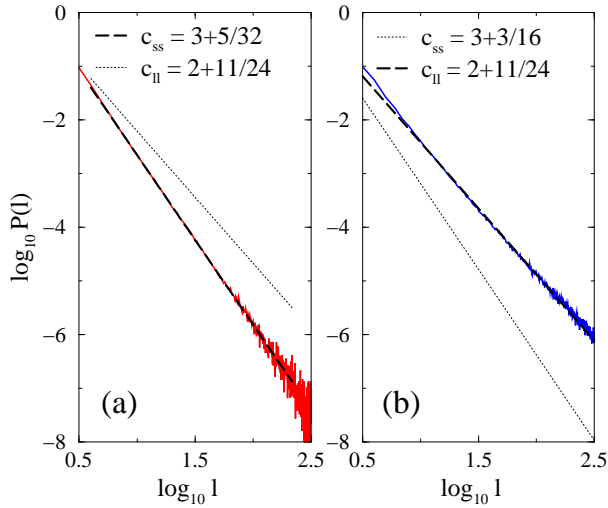
FIG. 8: Probability distribution of loop lengths at the estimated transition point $\beta = \beta_c = 1.7617$ (a) and in the high temperature phase $\beta = 1.6$ (b). As references we plot the exact exponents for a loop embedded between two segments $c_{ss} = 3 + 5/32$ and a loop embedded between two long loops $c_{ll} = 2 + 11/24$, calculated in the preceding section.
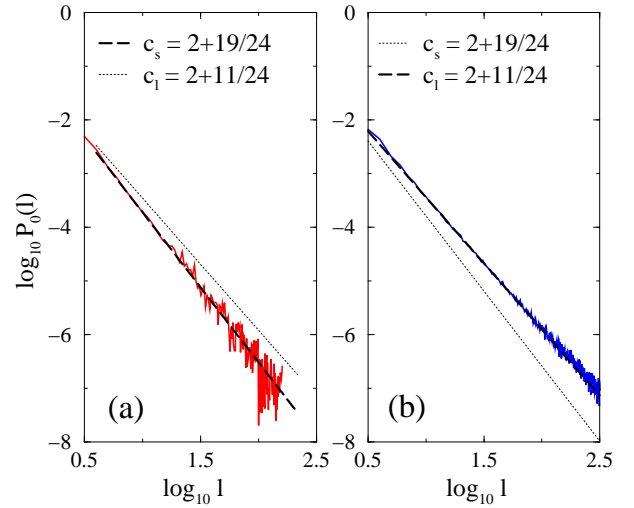

FIG. 9: Probability distribution of the first loop as a function of its length in a log-log scale at the estimated transition point $\beta = \beta_c = 1.7617$ (a) and in the high temperature phase $\beta = 1.6$ (b). The slopes corresponding to the analytical estimates for the exponents c_s and c_l for a loop bounded by a SAW segment and by another long loops are also shown.

of the two strands. Here we have considered only loops originated at the very edge for which the first monomer is unbound ($\vec{r}_1(1) \neq \vec{r}_2(1)$). A plot of $\log P_0(l)$ as a function of $\log l$ at β_c is shown in Fig. 9(a). The statistics is poorer compared to the total loop distribution in Fig. 8(a), as in most of the configurations the first monomer is bound, therefore loops at the common edge of the two strands are quite rare. Despite that, the agreement with the expected exponent $c_s = 2 + 19/24$ is very good.

Finally we considered the end-segments distribution which is shown in Fig. 10(a). Here $P_e(n)$ is the probability of having a configuration in which the last $n - 1$ monomers are unbound while $\vec{r}_1(n) = \vec{r}_2(n)$. Once again at β_c we note a good agreement with a decay $P_e(n) \sim n^{-\gamma_s}$ with an exponent $\gamma_s = 7/6$.

B. Behavior in the high temperature phase $\beta < \beta_c$

We have repeated the same type of calculation of loops and end-segments statistics also in the high temperature region $\beta < \beta_c$. We expect a power-law distribution of loop lengths also at high temperatures [5].

Figure 8(b) shows a plot of the loop probability distribution at $\beta = 1.6$ for $N = 1280$. Indeed there is a clear power-law decay governed by an exponent which is in excellent agreement with $c_{ll} = 2.46$ as calculated in the preceding section. Typically at high temperatures a loop is more likely to be bound by neighboring loops, rather than double stranded segments, as contacts between the two strands are rare, which explains the observed exponent.

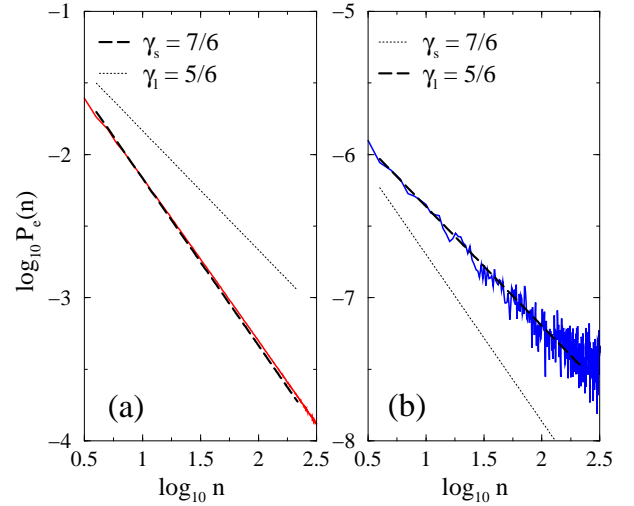Analogously, also for the first loop length distribution

FIG. 10: Probability distribution for the end segments at the estimated transition point $\beta = \beta_c = 1.7617$ (a) and in the high temperature region $\beta = 1.6$ (b). The analytical estimates γ_s and γ_l for the slopes for end segments attached to a SAW and to a loop respectively, are also shown.

$P_0(l)$, we find a decay exponent in very good agreement with c_l (see Fig. 9(b)). Notice that, differently from the $\beta = \beta_c$ case, here the distribution is rather smooth, as, in the high temperature region, it is more likely to find configuration where a loop forms at the origin.

An analogous very good agreement with the exponent γ_l has also been found for the decay of the end segments distribution $P_e(n)$, as illustrated in Fig. 10(b).

V. DISCUSSION

In this paper we have studied the unbinding transition for a two-dimensional lattice polymer composed of two strands which are random walks mutually avoiding each other. Considering all the polymer unbinding models studied so far in the literature in two and three dimensions, the present model is that with the strongest first order transition (higher loop exponent $c \approx 3.2$). The sharp first order behavior can be inferred from the determination of the crossover exponent ϕ, which is in excellent agreement with the first order value $\phi = 1$, already clearly observed for rather short chains ($N \approx 100$). This can be compared with, for instance, the unbinding for SAWs in three dimensions for which $c \approx 2.1$ (weak first order, just above the threshold $c = 2$) and numerical $\phi \sim 0.9$, in itself not fully consistent with a first order transition [3].

We showed that numerical estimates of entropic exponents for loops and end segments are in excellent agreement with analytical results, obtained from a recent theory based on mapping of star copolymers into a fluctuating geometry [12]. Such good agreement is not surprising in the high temperature phase where the loops are most likely bound by other loops as contacts between the strands are very rare. At the transition point one expects that typical configurations are composed by a double stranded polymer "dressed" with loops of all sizes. Notice however that as the loop exponent is rather large ($c \approx 3.2$), the statistical weight of long loops is suppressed. In particular $c > 3$ implies that the two first moments $\langle l \rangle$ and $\langle l^2 \rangle$ are finite. In this case, as loops are typically very small (see also Fig. 2), therefore neglecting totally their effect is still a very good approximation. Thus the strong first order unbinding represents an ideal case where polymer networks calculations work extremely well.

As a counterexample we mention the case of a two dimensional unbinding transition studied recently in diblock copolymers [24]. A diblock copolymer is composed by two homogeneous branches of A and B monomers joined at a common origin. In the model of Ref. [24] A and B are both self- and mutually avoiding. An attractive interaction between A and B induces a "zipping" transi-
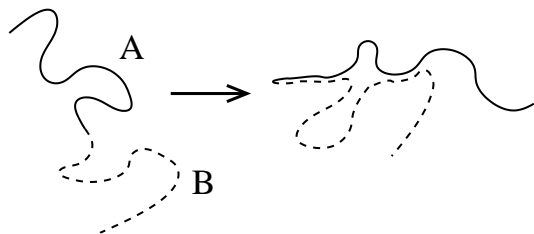

FIG. 11: Zipping transition for a two dimensional diblock copolymer. Both strands A and B are mutually and self-avoiding. Loops in the zipped phase may have different lengths in the two strands.

tion by lowering the temperature where the two strands are bound (see Fig. 11). Differently from the model studied here and in models of DNA denaturation [2, 3, 5, 8] any "monomer" in A can bind to any "monomer" in B, therefore loops of total length l may have different lengths along the two strands, i.e. $l = l_A + l_B$ with $l_A \neq l_B$. Due to this freedom the loop entropic exponents for the diblock copolymer are given by:

$$c_{\mathrm{ss}} = c_{\mathrm{ss}}^{\mathrm{(SAW)}} - 1 \approx 1.42 \tag{33}$$

$$c_{\mathrm{ll}} = c_{\mathrm{ll}}^{\mathrm{(SAW)}} - 1 \approx 1.64 \tag{34}$$

where we have used the two dimensional SAW exponents [2]: $c_{\mathrm{ss}}^{\mathrm{(SAW)}} = 2.42$ and $c_{\mathrm{ll}}^{\mathrm{(SAW)}} = 2.64$. Numerical results [24] shows that the zipping transition is continuous and the specific heat exponent is in excellent agreement with $\phi = 9/16$, conjectured to be an exact value. From scaling arguments for a continuous transition [5] one has $c = 1 + \phi = 25/16 \approx 1.56$, which is in between the values of Eqs. (33) and (34), clearly distinct from both. At the zipping transition therefore the polymer network theory does not reproduce the numerical value for the loops entropic exponent as accurately as for the model studied here. Notice that however, also in this case the numerically determined c satisfies the relation $c_{\mathrm{ss}} < c < c_{\mathrm{ll}}$, as expected.

APPENDIX A: STAR COPOLYMER MADE OF k MUTUALLY AVOIDING RANDOM WALKS

We generalize here the calculation leading to Eq. (12) to the case of consider a star copolymer S_k made of k mutually avoiding random walks. In this case the surface conformal dimension in the fluctuating geometry is k-times that of a single random walk [Eq. (4)]: $\widetilde{\Delta}^{\mathrm{qg}}(S_k) = k$. Using Eqs. (8) and (6) we find:

$$\Delta(S_k) = \frac{4k^2 - 1}{24} \tag{A1}$$

which correctly reproduces $\Delta(S_a)$ of Eq. (12) for $k = 2$. In the case of four mutually avoiding walks

$$\Delta(S_4) = \frac{21}{8} \tag{A2}$$

Notice that the vertex S_c of Fig. 4 is also formed by four random walks, however not all mutually avoiding and its bulk conformal dimension is $\Delta(S_c) = 35/24 < \Delta(S_4)$. $\Delta(S_c)$ is smaller as more configurations are available for the star copolymer when partial overlapping between

walks is allowed, as in S_c. Had we put no restrictions on the order of the loops in the construction of the model both vertices S_c and S_4 would have been generated. It should be emphasized that for two dimensional star copolymers the order of the constituing walks does matter.

[1] D. Cule and T. Hwa, Phys. Rev. Lett. **79**, 2375 (1997).

[2] Y. Kafri, D. Mukamel, and L. Peliti, Phys. Rev. Lett. **85**, 4988 (2000).

[3] M. S. Causo, B. Coluzzi, and P. Grassberger, Phys. Rev. E **62**, 3958 (2000).

[4] T. Garel, C. Monthus, and H. Orland, Europhys. Lett. **55**, 132 (2001).

[5] E. Carlon, E. Orlandini, and A. L. Stella, Phys. Rev. Lett. **88**, 198101 (2002).

[6] M. Barbi, S. Lepri, M. Peyrard, and N. Theodorakopoulos, Phys. Rev. E **68**, 061909 (2003).

[7] M. Peyrard and A. R. Bishop, Phys. Rev. Lett. **62**, 2755 (1989).

[8] D. Poland and H. A. Scheraga, J. Chem. Phys. **45**, 1456 (1966).

[9] M. E. Fisher, J. Chem. Phys. **44**, 616 (1966).

[10] B. Duplantier, Phys. Rev. Lett. **57**, 941 (1986).

[11] M. Baiesi, E. Carlon, and A. L. Stella, Phys. Rev. E **66**, 021804 (2002).

[12] B. Duplantier, Phys. Rev. Lett. **82**, 880 (1999).

[13] C. Vanderzande, *Lattice Models of Polymers* (Cambridge University Press, Cambridge, 1998).

[14] M. Baiesi, E. Carlon, E. Orlandini, and A. L. Stella, Eur. Phys. J. B **29**, 129 (2002).

[15] P. Grassberger, Phys. Rev. E **56**, 3682 (1997).

[16] C. von Ferber and Y. Holovatch, Phys. Rev. E **56**, 6370 (1997).

[17] B. Duplantier, J. Stat. Phys. **110**, 691 (2003).

[18] V. G. Knizhnik, A. M. Polyakov, and A. B. Zamolodchikov, Mod. Phys. Lett. **A3**, 819 (1988).

[19] B. Duplantier, Phys. Rev. Lett. **81**, 5489 (1998).

[20] C. von Ferber and Y. Holovatch, Phys. Rev. E **59**, 6914 (1999).

[21] This corrects an error of Ref. [14] where the value 3+7/16 was reported.

[22] Y. Kafri, D. Mukamel, and L. Peliti, Eur. Phys. J. B **27**, 132 (2002).

[23] A. M. Ferrenberg, and R. H. Swendsen, Phys. Rev. Lett. **61**, 2635 (1988); **63**, 1195 (1989).

[24] M. Baiesi, E. Carlon, E. Orlandini, and A. L. Stella, Phys. Rev. E **63**, 041801 (2001).